DNA Cleaving "Tandem-Array" Metallopeptides Activated With KHSO$_5$: Towards the Development of Multi-Metallated Bioactive Conjugates and Compounds

Mark A. Lewis[1], **Katie M. Williams**[1], **Ya-Yin Fang**[2], **Franklin A. Schultz**[1], and **Eric C. Long**[1,*]

[1]Department of Chemistry & Chemical Biology, Indiana University-Purdue University Indianapolis (IUPUI), Indianapolis, Indiana 46202

[2]Department of Biochemistry & Molecular Biology, Howard University, 520 W Street, NW, Washington, D. C. 20059

Abstract

Amino terminal peptides of the general form Gly-Gly-His have been used to introduce single sites of metal binding and redox activity into a wide range of biomolecules to create bioactive compounds and conjugates capable of substrate oxidation. We report here that Gly-Gly-His-like peptides linked in a tandem fashion can also be generated leading to multi-metal binding arrays. While metal binding by the native Gly-Gly-His motif (typically to Cu^{2+}, Ni^{2+}, or Co^{2+}) requires a terminal peptide amine ligand, previous work has demonstrated that an ornithine (Orn) residue can be substituted for the terminal Gly residue to allow solid-phase peptide synthesis to continue via the side chain *N*-δ. This strategy thus frees the Orn residue *N*-α for metal binding and permits placement of a Gly-Gly-His-like metal binding domain at any location within a linear, synthetic peptide chain. As we show here, this strategy also permits the assembly of tandem arrays of metal binding units in linear peptides of the form: NH$_2$-Gly-Gly-His-[(δ)-Orn-Gly-His]$_n$-(δ)-Orn-Gly-His-CONH$_2$ (where $n = 0, 1,$ and 2). Metal binding titrations of these tandem arrays monitored by UV-vis and ESI-MS indicated that they bind Cu^{2+}, Ni^{2+}, or Co^{2+} at each available metal binding site. Further, it was found that these systems retained their ability to modify DNA oxidatively and to an extent greater than their parent M(II)•Gly-Gly-His. These findings suggest that the tandem array metallopeptides described here may function with increased efficiency as "next generation" appendages in the design of bioactive compounds and conjugates.

Keywords

DNA cleavage; metallopeptide; Gly-Gly-His; metal binding peptide

*Address correspondence to this author at the Department of Chemistry & Chemical Biology, Indiana University-Purdue University Indianapolis (IUPUI), 402 North Blackford Street, Indianapolis, IN 46202-3274; Tel: (317) 274-6888; Fax: (317) 274-4701; eclong@iupui.edu.

CONFLICT OF INTEREST The authors confirm that this article content has no conflict of interest.

INTRODUCTION

Amino terminal peptides of the general form Gly-Gly-His provide a strategy to introduce sites of metal binding and redox activity into a wide range of biomolecules to create compounds and conjugates capable of substrate oxidation [1]. We report here that tandem arrays of these metal binding units can also be synthesized leading to multi-metallated linear peptides capable of increased substrate oxidation. The basis for these tandem arrays, the parent Gly-Gly-His peptide system, was developed originally as a model of the amino-terminal, square planar Cu(II)-chelating domain of the serum albumins [2]; these systems are known to bind Cu^{2+} and Ni^{2+} tightly with K_D values in the range $10^{-16} - 10^{-17}$ [2,3] to form 1:1 complexes at physiological pH or above through metal chelation by the terminal peptide amine, two intervening deprotonated peptide amides, and the His imidazole ring (Fig. **1**). Upon metal binding, these systems can be activated toward the oxidative modification of an associated substrate, *e.g.*, nucleic acid strand scission or protein cleavage/crosslinking [1]. Indeed, the discovery of their ability to effect the oxidative modification of substrates [4,5] has led to the exploitation of these tripeptides as synthetic [6–9] or biosynthetic [10,11] conjugates to DNA-targeted proteins and a range of additional biomolecules including peptides [12], low molecular weight drugs [13–15], oligonucleotides [16,17], PNA strands [18], and protein-targeted systems [19–22]. More recently, Gly-Gly-His has provided a basis for the development of catalytic metallodrugs [23, 24].

Due to the requirement of a terminal peptide amine in the coordination of metal ions, the placement of a native Gly-Gly-His motif is limited to single, isolated units at the amino-termini of peptides and proteins. This restriction thus decreases the versatility of this motif in the development of additional bioactive compounds and seemingly eliminates the possible incorporation of multiple metal-binding units in close proximity. To circumvent the need for a terminal peptide amine, a synthetic strategy was developed in this laboratory a number of years ago that permits a synthetic peptide to retain the metal binding, electronic, and reactive properties of Gly-Gly-His while also permitting its positioning at any location within a linear peptide chain [25,26]. In this strategy, substitution of an appropriately protected ornithine (Orn) residue for amino terminal Gly_1, followed by selective on-resin deprotection of the Orn side chain *N*-δ, permits solid-phase peptide synthesis to continue via a (δ)-Orn coupling while freeing the Orn *N*-α to participate in creating a four coordinate metal binding site in the final peptide (Fig. **1**). This protocol thus allows placement of a Gly-Gly-His-like metal binding motif at amino-terminal, interior, or carboxy-terminal positions within synthetic peptides.

Exploiting this earlier work, we now report that multiple units of Orn-Gly-His metal-binding domains can be conjugated into tandem arrays as a possible strategy to increase the efficiency of substrate modification. Our design led to the synthesis of model peptides (Fig. **1**) where two-to-four metal binding domains were linked together in the sequence NH_2-Gly-Gly-His-[(δ)-Orn-Gly-His]$_n$-(δ)-Orn-Gly-His-$CONH_2$ (where n = 0, 1, or 2). In each case, the α-amino group of every Orn residue is available to participate in metal ligation in a fashion analogous to that of free terminal amine of Gly-Gly-His [1–3]. As will be shown, tandem array peptides of multiple (δ)-Orn-Gly-His units can indeed bind Cu^{2+}, Ni^{2+}, or Co^{2+} at all available metal binding sites and remain competent to induce oxidative DNA

strand scission (in the presence of Ni^{2+} and $KHSO_5$). Our results also indicate that these tandem array systems, as expected, are more efficient at inducing substrate modification relative to an equimolar amount of individual, non-linked metallotripeptide. Thus, these systems are capable of binding multiple metals and can be employed as synthetic bioconjugates analogous to the parent Gly-Gly-His tripeptide, albeit with increased potency.

MATERIALS AND METHODS

Peptide Synthesis

All peptides utilized in this study were synthesized manually using routine solid-phase protocols [27] and commercially available (Bachem) Fmoc-protected L-amino acids and Rink resin (200–400 mesh). For steps involving an Orn coupling, N-δ-Fmoc-N-α-Boc-L-Orn was used to permit selective deprotection of the N-δ-position during main-chain assembly to allow continued peptide coupling via this position in lieu of the N-α of this residue. Fmoc deprotections were carried out using 30% piperidine/70% DMF while amino acid activation and peptide coupling employed HOBT and diisopropylcarbodiimide. Peptides employed in quantitative titration experiments were synthesized with a carboxy-terminal Tyr residue that provided a spectroscopic tag for accurate peptide quantitation (via $\varepsilon_{275} = 1500$ cm^{-1}M^{-1}) [28]. Side chain deprotections and resin cleavages were accomplished using 95% TFA/H_2O. Peptides were confirmed by reverse-phase HPLC and ESI-LCMS (Agilent 1100 Series) using a 10 min linear gradient starting with 100% H_2O containing 0.1% TFA and completing with 95% acetonitrile containing 0.1% TFA. Values for m/z observed (calculated) were: Gly-Gly-His-Tyr, **1**, 432.1 (431); Gly-Gly-His-(δ)-Orn-Gly-His-Tyr, **2**, 740.2 (740); Gly-Gly-His-(δ)-Orn-Gly-His-(δ)-Orn-Gly-His-Tyr, **3**, 1048.3 (1048); Gly-Gly-His-(δ)-Orn-Gly-His-(δ)-Orn-Gly-His-(δ)-Orn-Gly-His-Tyr, **4**, 1357.3 (1356)]. Bulk purifications were carried out using HPLC and the solvent system noted above.

UV-Visible Spectroscopy

UV-visible absorbance titrations to assess the stoichiometry of peptide-metal binding were carried out using a Perkin Elmer UV/Vis/NIR Lambda 19 spectrophotometer and 1.0 mL quartz cuvettes containing 40 mM Na-cacodylate buffer, pH 7.4, and 1.0 mM peptide. Concentrated aqueous stocks of Cu^{2+} or Ni^{2+} were prepared gravimetrically from their respective chloride salts, diluted appropriately, and titrated as 3 μL aliquots into each cuvette. Sample absorbances were measured after each aliquot addition and mixing; samples were scanned or measured at $\lambda_{max} = 420$ nm and at $\lambda_{max} = 525$ nm for the Ni^{2+} and Cu^{2+} titrations, respectively. In the examination of the stoichiometry of Co-peptide binding by UV-vis, peptide samples were prepared as buffered 0.5 mM solutions (Tris, pH 8.0, at 7 mM and 11 mM for peptides **1** and **2**, respectively, and 15 mM for peptides **3** and **4**), purged with O_2 gas, treated with aliquots of freshly prepared, O_2-purged $CoCl_2$ and stirred at room temperature overnight; these Co(III)•metallopeptide samples were scanned from 300 to 700 nm or monitored at 430 nm for titrations.

ESI-Mass Spectrometry

ESI-MS analyses of Cu^{2+}- and Ni^{2+}-peptides (**4**) were carried out using preformed metallopeptides (in 40 mM Tris buffer, pH 7.4) of varied metal binding site to metal ion

ratios, *e.g.*, 4:1, 4:2, 4:3 and 4:4. Preformed metallopeptides were added to a solution of 50% acetonitrile/40 mM Tris buffer, pH 7.4, followed by analysis using an octapole LCQ mass spectrometer (SN 000002). LCQ tune and Excalibur software were used to analyze the *m/z* spectra; calculated spectra were obtained via a mass isotope calculator.

DNA Cleavage

DNA cleavage analyses were carried out by pre-metallating stocks of Gly-Gly-His, Gly-Gly-His-(δ)-Orn-Gly-His and Gly-Gly-His-(δ)-Orn-Gly-His-(δ)-Orn-Gly-His with Ni(OAc)$_2$ at a ratio of metal to metal binding site of 1:1 (*i.e.*, 1:1 metal:peptide for Gly-Gly-His and 2:1 metal:peptide for Gly-Gly-His-(δ)-Orn-Gly-His) in 17 mM Na-cacodylate buffer, pH 7.5. Aliquot volumes appropriate for the desired final reaction concentrations were dispensed from these preformed metallopeptide stocks into Eppendorf tubes, followed by the addition of ΦX174 RF DNA (30 μM base pair final concentration). After incubating all DNA + metallopeptide mixtures for 10 min at room temperature, cleavage reactions were initiated through the addition of aliquots of a freshly prepared aqueous solution of KHSO$_5$ [29] to the final desired concentration and to complete the final reaction volume (20 μL) in 10 mM Na-cacodylate, pH 7.5. All reactions were quenched after 1 min through the addition of an EDTA-containing (15 mM final concentration) agarose gel loading buffer. Reaction aliquots were loaded into 0.9% agarose gels containing 0.5 μg/mL ethidium bromide and electrophoresed in TAE buffer at 100 volts for 2 h. Gels were visualized using a Bio-Rad Gel Doc system coupled to image analysis software. Quantitation of supercoiled Form I and nicked-circular Form II DNAs was carried out via a densitometric analysis, applying a correction factor of 1.47 to account for the reduced binding of ethidium bromide to Form I DNA.

Molecular Modeling and Simulations

Molecular modeling and simulations were carried out on the Ni(II)$_4$•Gly-Gly-His-(δ)-Orn-Gly-His-(δ)-Orn-Gly-His-(δ)-Orn-Gly-His system using the following software packages: *SPARTAN '02* [30], *Sybyl* 7.2 [31], *MacroModel 7.0* [32], and *AMBER 7* [33]. Default settings for these programs were used unless specified otherwise. The metal bound Ni(II)$_4$•Gly-Gly-His-(δ)-Orn-Gly-His-(δ)-Orn-Gly-His-(δ)-Orn-Gly-His system was developed from the atomic coordinates of the basic Ni(II)•Gly-Gly-His metallopeptide; procedures for this process and the development of missing force field parameters have been described [34]. The multi-metal binding system was assembled beginning with individual Ni(II)•Gly-Gly-His metallopeptides that were transformed into Ni(II)•Orn-Gly-His units by adding an Orn side chain to the first amino acid position using the automatic adding function in *SPARTAN '02*. The multi-metal binding metallopeptide was then generated via the XLEaP facility of *AMBER* by connecting three individual Ni(II)•Orn-Gly-His units via peptide bonds and concluding with the connection of an amino-terminal Ni(II)•Gly-Gly-His. The previously developed force field parameters [34] for the basic Ni(II)•Gly-Gly-His unit were adapted to the new multi-metal binding system and the atomic charges were obtained through single point energy calculations of the assembled complex in *SPARTAN '02*. The multi-metal binding system was then solvated explicitly using the TIP3P water potential inside a central simulation box; the box dimensions chosen ensured that solvation extended 10 Å on all sides of the embedded multi-metal binding system. Subsequent MD simulations

were carried out as described previously [34] with production runs in excess of 5000 ps. Structures (25,000) were saved to disk during the simulation for post-processing by uniformly sampling the trajectory during the production run. All analyses of results were performed using the CARNAL and ANAL programs in *AMBER*.

RESULTS AND DISCUSSION

Peptide Design and Synthesis

Using the strategy outlined in Figure **1** and standard Fmoc-based solid phase peptide synthesis protocols, four model peptides were assembled containing one, two, three, or four Gly-Gly-His-like metal binding units, respectively: Gly-Gly-His-Tyr, **1**; Gly-Gly-His-(δ)-Orn-Gly-His-Tyr, **2**; Gly-Gly-His-(δ)-Orn-Gly-His-(δ)-Orn-Gly-His-Tyr, **3**; and Gly-Gly-His-(δ)-Orn-Gly-His-(δ)-Orn-Gly-His-(δ)-Orn-Gly-His-Tyr, **4**. Each peptide was synthesized containing a carboxamide-terminal Tyr residue to facilitate accurate peptide quantification via Tyr absorbance [28]; additional peptides without a terminal Tyr residue were synthesized in parallel. In the case of **1**, the peptide contained an amino-terminal Gly-Gly-His motif in the native metal binding environment and served as a control and standard for comparison throughout our study. All syntheses employed established Fmoc procedures and commercially-available, protected amino acid monomers; individual couplings proceeded smoothly as reported also for earlier studies that employed tBoc protocols to incorporate (δ)-Orn-Gly-His into linear peptide chains [25,26].

UV-Vis Spectrophotometric Analyses of Metal Binding

Peptides **1**–**4** were analyzed by UV-vis spectrophotometry to assess their ability to bind transition metals and to determine whether or not they did so stoichiometrically based on the number of available Gly-Gly-His-like metal binding units. As illustrated for peptide **4** (Fig. **2**, top panels), when 1 mM of peptide was titrated with Cu^{2+} or Ni^{2+}, and monitored within the range of their expected λ_{max} values (525 nm and 420 nm indicative of Cu^{2+} and Ni^{2+}-bound Gly-Gly-His motifs, respectively) [1–3], metal binding was indeed observed. Metal binding was also observed to saturate upon full occupancy of each peptide (*e.g.*, four equivalents of M^{2+} for **4**); additional equivalents of metal ion beyond full saturation did not result in increased sample absorbance for any peptide studied. As also illustrated (Fig. **2**, top panels), the UV-vis spectra of peptide **4** titrated with Cu^{2+} or Ni^{2+} indicated that intermediate titration points all display spectral characteristics identical to that of the isolated, native amino-terminal Gly-Gly-His control peptide **1** when bound to Cu or Ni; shifts in the λ_{max} of **4** upon metal binding were not observed relative to M(II)•**1** nor evidence of hypo- or hyperchromicity. The λ_{max} values and extinction coefficients determined for these species were the same under our conditions. Indeed, it was found that Gly-Gly-His-Tyr, **1**, bound Cu^{2+} in a 1:1 stoichiometric ratio and exhibited λ_{max} (525 nm) and molar extinction coefficient (90 $M^{-1}cm^{-1}$) values that were identical to the λ_{max} and molar extinction coefficients for $Cu(II)_2$•**2**, $Cu(II)_3$•**3**, and $Cu(II)_4$•**4**, on a per metal binding site basis; these values are comparable to literature values [2,3,25,26]. Similarly, **1** bound to Ni^{2+} with a λ_{max} of 420 nm and exhibited a molar extinction coefficient of 98 $M^{-1}\ cm^{-1}$ while the λ_{max} and molar extinction coefficients for $Ni(II)_2$•**2**, $Ni(II)_3$•**3**, and $Ni(II)_4$•**4**, again on a per metal binding site basis, were found to be similar to each other and to literature

values [2]. The linearity of the observed absorbance with respect to the concentration of available metal binding sites suggests that each metal binding site behaves in a fashion similar to an isolated, metal-bound Gly-Gly-His unit.

As a further assessment of the metal binding stoichiometries of these systems, 1 mM of each peptide (**1**–**4**) was titrated with Cu^{2+} or Ni^{2+}, and monitored at their respective λ_{max} values (525 nm and 420 nm, respectively) indicative of the metal-bound peptides (Fig. **2**, middle panels). With each model peptide, metal binding was observed to plateau upon attainment of full stoichiometric occupancy of all Gly-Gly-His-like motifs present in a given peptide. The slight deviations observed from uniformity in the final incremental absorbances attained upon metal binding to the four different peptide samples at saturation were found to be within experimental error. Consistent with the extinction coefficients presented earlier, the total absorbance of 1 mM $Cu(II)_4$•**4** (Fig. **2**) was found to be identical to 4 mM $Cu(II)$•**1**. Further, given the overlapping slopes of each titration plot illustrated in Fig. **2**, it is apparent that each available metal binding system exhibited an affinity for a given metal ion that was comparable to the parent control peptide **1** [3] under identical conditions. This result is in accord with previous studies of Orn-Gly-His metal binding [25,26] and supports the notion that each metal binding site is minimally impacted by the proximity of a flanking site. Thus, based on the results described above, it appears that each model peptide was capable of binding Cu^{2+} and Ni^{2+} stoichiometrically in a tetradentate manner based on the number of available Gly-Gly-His-like units.

Along with analyses of Cu^{2+} and Ni^{2+} binding, the formation of Co(III)-bound tandem array peptides was also examined. With these systems, Co^{2+} salts were employed to metallate each peptide structure followed by *in situ* O_2 oxidation to generate Co(III)-bound metallopeptides that were analyzed subsequently by UV-vis absorbance spectroscopy. Complete oxidation of peptide-bound Co^{2+} to Co^{3+} provides a uniform basis through which to monitor and compare metal binding to earlier systems [35,36]. This protocol was employed also in the generation of monomeric Co(III)•Gly-Gly-His metallopeptides [35,36]. As shown in Figure **2**, the final Co(III)-metallated tandem array peptide **4** exhibited absorbance in the visible region of the spectrum (with a maximum at 430 nm and a broader absorbance between 522–546 nm) consistent with Co-peptide coordination. These spectral features are analogous to those reported previously for Co(III)•Gly-Gly-His (λ_{max} values at 434 nm and 520 nm [35,36] and $(NH_3)_2$Co(III)•Gly-Gly-His-COOH (λ_{max} values at 442 nm and 520 nm) [37]. Thus, as observed with Cu and Ni, Co was found to bind stoichiometrically to these systems (**1**–**4**) based on the number of available Gly-Gly-His-like motifs: metal binding attained a saturation point at 1:1 Co:metal binding site and further equivalents of added Co^{2+} (+ O_2) did not influence the spectra.

ESI-MS Analyses of Metal Binding

The metal binding of our tandem array system was investigated further using ESI-MS. Employing peptide **4**, containing four tandem-linked Gly-Gly-His-like motifs, preformed metal-peptide complexes were generated by combining the apo-peptide with one, two, three, or four equivalents of Cu^{2+} (or Ni^{2+}) in 40 mM Tris buffer, pH 7.4; these metallated peptides were then analyzed by ESI-MS. As shown in Figure **3** for a metal:metal binding

site ratio of 3:4 (chosen to illustrate the presence of all species), five major clusters of m/z values (1356.6, 1417.5, 1478.2, 1542.2, and 1605.2) were found. These values correspond to apo peptide **4**, Cu(II)•**4**, Cu(II)$_2$•**4**, Cu(II)$_3$•**4**, and Cu(II)$_4$•**4**, respectively, and provide direct evidence for the binding of multiple metals simultaneously. Further, close analysis of m/z values clustered around $m/z = 1417.5$ indicate that the values present in the cluster correspond exactly to the predicted isotopic distribution for peptide **4** bound to a single Cu (shown as an expansion in Fig. **3**). For analyses carried out at a metal to metal binding site ratio of 4:4, the m/z value of 1605 was found to predominate, while analyses of samples containing lower added equivalents of metal ion (1:4 and 2:4) permitted observation of the gradual disappearance of apo-peptide accompanied by the appearance of species of intermediate metal binding occupancy. Along with the Cu(II)-bound systems, the ESI-MS of Ni^{2+} bound to **4** was analyzed in an identical fashion; the values observed indicated the ability of **4** to bind Ni^{2+} stoichiometrically as observed with Cu^{2+} (data not shown).

The above analyses confirmed that peptides **2**–**4** are capable of binding to Cu^{2+} and Ni^{2+} to form linear arrays of tetrachelated, square-planar, or distorted square planar structures. In addition, as demonstrated with Co, these peptides can also accommodate to full occupancy transition metal ions that ultimately metallate the peptides in an exchange-inert fashion with final octahedral geometries.

Modeling and Simulation

To examine the likely solution structure and behavior of the multiple metal binding system described above, we carried out molecular simulations and modeling of Ni(II)$_4$•Gly-Gly-His-(δ)-Orn-Gly-His-(δ)-Orn-Gly-His-(δ)-Orn-Gly-His. Using the crystal structure of a monomeric system as a starting point [38], molecular dynamics (MD) simulations were carried out as described previously [34] with production runs in excess of 5000 ps. Initially, the root mean square deviation (RMSD) observed in the simulation of this system was examined to determine if the system had attained equilibrium; the RMSD of the oligomer-complex with respect to its starting structure was determined to attain equilibrium after 250 ps and the energy was found to be stable during the course of the remainder of the simulation. Hence, a time of 500 ps after thermal warm-up was selected as a starting point for data collection and analysis of the simulation trajectory.

Visual analysis of the 5 ns simulation trajectory indicated that the linear, metallated oligomer fluctuated from an extended conformation to a folded, hairpin conformation. As an evaluation of these conformational changes, the distance between the Ni ions at each terminus of the four metal-containing system was monitored and found to alternate between ~ 32 Å in the most extended structures to ~ 12 Å in the folded, hairpin conformation; these same Ni atoms were ~ 20 Å apart in the starting structure. In the final analysis approximately 10% of the total snapshots obtained during the course of the simulation revealed the two terminal Ni atoms to be < 15 Å apart, with 22% of the structures folded to < 18 Å apart. Overall, the average structure of this system (Fig. **4**) revealed that the total length of the oligomer was approximately 23 Å and that the individual metal binding equatorial planes were extended away from each other during most instances. While only speculation at this point, close examination of these models suggested that the flexibility and

extended nature of this system may enable it to closely align with the structure of a DNA minor groove, an established target for monomeric M(II)•Gly-Gly-His metallopeptides [1,29,34,39,40], perhaps as a consequence promoting association within the minor groove and the interaction of multiple metals simultaneously with the DNA target.

Assessment of Reactivity via DNA Cleavage Activity

Having confirmed the ability of peptides **2**–**4** to bind multiple equivalents of Cu, Ni, and Co, the impact of metal binding site linkage on the reactivity of these systems was assessed in comparison to monomeric M(II)•Gly-Gly-His units through a test of their DNA cleavage competence [29,34]. It is well established that Ni(II)•Gly-Gly-His peptides can be activated oxidatively to cleave DNA through the use of $KHSO_5$ or other agents [29,34,39]; a standard test for the ability of such agents to cleave DNA involves monitoring the conversion of supercoiled (Form I) plasmid DNA into cleaved, nicked-circular (Form II) DNA and linear (Form III) DNA [25]. As shown in Figure **5**, a side-by-side comparison of the ability of Ni(II)•Gly-Gly-His, Ni(II)$_2$•Gly-Gly-His-(δ)-Orn-Gly-His and Ni(II)$_3$•Gly-Gly-His-(δ)-Orn-Gly-His-(δ)-Orn-Gly-His to convert supercoiled Form I DNA to nicked-circular Form II DNA upon activation with $KHSO_5$ [29,34] indicated that Ni(II)$_2$•Gly-Gly-His-(δ)-Orn-Gly-His and Ni(II)$_3$•Gly-Gly-His-(δ)-Orn-Gly-His-(δ)-Orn-Gly-His remained active towards DNA cleavage in a fashion similar to Ni(II)•Gly-Gly-His; while Form II DNA was formed exclusively in this particular analysis, linear, Form III DNA was observed at higher metallopeptide concentrations (data not shown). Interestingly, a comparison of lanes 6, 7 and 8 indicated that the Orn-linked systems consistently cleaved DNA to an extent greater than Ni(II)•Gly-Gly-His *on a per metal basis*; each of these lanes contained an identical amount of Ni-bound peptide. Indeed, densitometric analysis of the DNA cleavage induced by Ni(II)$_3$•Gly-Gly-His-(δ)-Orn-Gly-His-(δ)-Orn-Gly-His indicated the generation of 64% Form II DNA, compared to 53% and 43% for Ni(II)$_2$•Gly-Gly-His-(δ)-Orn-Gly-His and Ni(II)•Gly-Gly-His, respectively. While this increased efficiency may simply be due to the greater capacity of the oligomeric system to interact with the target DNA relative to the monomeric system (as also noted during modelling), more importantly this result confirms that the environment provided by tandem-linked Orn-Gly-His units remains conducive to activation and substrate oxidative modification and that the oligomeric systems might function more efficiently than monomeric Gly-Gly-His upon conjugation to other entities.

CONCLUSIONS

Tandem-linked units of (δ)-Orn-Gly-His peptides can be synthesized conveniently through standard Fmoc solid phase methodologies and bind Cu, Ni, and Co in linear arrays that achieve full stoichiometric occupancy of the available Gly-Gly-His-like metal binding sites. While oligopeptides that specifically contain between two and four metal binding units were examined herein, the procedures employed, and the metallation propensities observed, appear amenable to the generation of longer metallated oligomers. Further, each tandem-linked (δ)-Orn-Gly-His unit appears to bind to a metal in a fashion similar to an amino-terminal Gly-Gly-His motif and individual (δ)-Orn-Gly-His sequences. Thus, like their monomeric counterparts, these multi-metallated systems may find utility in the development of bioconjugates with increased capacity to modify a bound substrate.

Acknowledgments

REFERENCES

[1]. Long, EC.; Claussen, CA. DNA and RNA Binders: From Small Molecules to Drugs. Demeunynk, M.; Bailly, C.; Wilson, WD., editors. Wiley-VCH; New York: 2003. p. 88-125.

[2]. Harford K, Sarkar B. Amino terminal Cu(II)- and Ni(II)-binding (ATCUN) motif of proteins and peptides: metal binding, DNA cleavage, and other properties. Acc. Chem. Res. 1997; 30:123–130.

[3]. Kozlowski H, Bal W, Dyba M, Kowalik-Jankowska T. Specific structure-stability relations in metallopeptides. Coord. Chem. Rev. 1999; 184:319–346.

[4]. Chiou S-H. DNA- and protein-scission activities of ascorbate in the presence of copper ion and a copper-peptide complex. J. Biochem. 1983; 94:1259–1267. [PubMed: 6654857]

[5]. Chiou S-H. DNA-scission activities of ascorbate in the presence of metal chelates. J. Biochem. 1984; 96:1307–1310. [PubMed: 6394599]

[6]. Dervan PB. Characterization of protein-DNA complexes by affinity cleaving. Methods Enzymol. 1991; 208:497–515. [PubMed: 1779845]

[7]. Mack DP, Iverson BL, Dervan PB. Design and chemical synthesis of a sequence-specific DNA cleaving protein. J. Am. Chem. Soc. 1988; 110:7572–7574.

[8]. Mack DP, Dervan PB. Nickel-mediated sequence-specific oxidative cleavage of DNA by a designed metalloprotein. J. Am. Chem. Soc. 1990; 112:4604–4606.

[9]. Mack DP, Dervan PB. Sequence-specific oxidative cleavage of DNA by a designed metalloprotein, Ni(II)•GGH(Hin139-190). Biochemistry. 1992; 31:9399–9405. [PubMed: 1390723]

[10]. Nagaoka M, Hagihara M, Kuwahara J, Sugiura Y. A novel zinc finger-based DNA cutter: biosynthetic design and highly selective DNA cleavage. J. Am. Chem. Soc. 1994; 116:4085–4086.

[11]. Harford C. Narindrasorasak, S.; Sarkar, B. The designed protein M(II)•Gly-Lys-His-Fos(138–211) specifically cleaves the AP-1 binding site containing DNA. Biochemistry. 1996; 35:4271–4278. [PubMed: 8605175]

[12]. Shullenberger DF, Long EC. Design and synthesis of a DNA-cleaving metallopeptide. Bioorg. Med. Chem. Lett. 1993; 3:333–336.

[13]. Grokhovsky SL, Nikolaev VA, Zubarev VE, Surovaya AN, Zhuze AL, Chernov BK, Sidorova N, Zasedatelev AS. Sequence-specific cleavage of DNA by netropsin analog containing a copper(II)-chelating peptide Gly-Gly-His. Mol. Biol. (Moscow, Russ. Fed., Engl. Ed.). 1992; 26:1274–1297.

[14]. Morier-Teissier E, Boitte N, Helbecque N, Bernier JL, Pommery N, Duvalet JL, Fournier C, Hecquet B, Catteau JP, Henichart JP. Synthesis and antitumor properties of an anthraquinone bisubstituted by the copper chelating peptide Gly-Gly-L-His. J. Med. Chem. 1993; 36:2084–2090. [PubMed: 8340911]

[15]. Steullet V, Dixon DW. Design, synthesis and DNA-cleavage of Gly-Gly-His-naphthalene diimide conjugates. Bioorg. Med. Chem. Lett. 1999; 9:2935–2940. [PubMed: 10571151]

[16]. De Napoli L, Messere A, Montesarchio D, Piccialli G, Benedetti E, Bucci E, Rossi F. A new solid-phase synthesis of oligonucleotides 3′-conjugated with peptides. Bioorg. Med. Chem. Lett. 1999; 7:395–400.

[17]. Truffert J-C, Asseline U, Brack A, Thuong NT. Synthesis, purification and characterization of two peptide-oligonucleotide conjugates as potential artificial nucleases. Tetrahedron. 1996; 52:3005–3016.

[18]. Footer M, Egholm M, Kron S, Coull JM, Matsudaira P. Biochemical evidence that a D-loop is part of a four-stranded PNA-DNA bundle. Nickel-mediated cleavage of duplex DNA by a Gly-Gly-His bis-PNA. Biochemistry. 1996; 35:10673–10679. [PubMed: 8718856]

[19]. Cuenoud B, Tarasow TM, Schepartz A. A new strategy for directed protein cleavage. Tetrahedron Lett. 1992; 33:895–898.

[20]. Brown KC, Yu Z, Burlingame AL, Craik CS. Determining protein-protein interactions by oxidative cross-linking of a glycine-glycine-histidine fusion protein. Biochemistry. 1998; 37:4397–4406. [PubMed: 9521759]

[21]. Van Dijk J, Lafont C, Knetsch MLW, Derancourt J, Manstein DJ, Long EC, Chaussepied P. Conformational changes in actin-myosin isoforms probed by Ni(II)•Gly-Gly-His reactivity. J. Muscle Res. Cell Motil. 2004; 25:527–537. [PubMed: 15711883]

[22]. Brown K, Yang S-H, Kodadek T. Highly specific oxidative cross-linking of proteins mediated by a nickel-peptide complex. Biochemistry. 1995; 34:4733–4739. [PubMed: 7718579]

[23]. Hocharoen L, Joyner JC, Cowan JA. N-versus C-domain selectivity of catalytic inactivation of human angiotensin converting enzyme by lisinopril-coupled transition metal chelates. J. Med. Chem. 2013; 56:9826–9836. [PubMed: 24228790]

[24]. Joyner JC, Hodnick WF, Cowan AS, Tamuly D, Boyd R, Cowan JA. Antimicrobial metallopeptides with broad nuclease and ribonuclease activity. Chem. Comm. 2013; 49:2118–2120. [PubMed: 23380915]

[25]. Shullenberger DF, Eason PD, Long EC. Design and synthesis of a versatile DNA-cleaving metallopeptide structural domain. J. Am. Chem. Soc. 1993; 115:11038–11039.

[26]. Long, EC.; Eason, PD.; Shullenberger, DF. Metal-Containing Polymeric Materials. Carraher, CE.; Zeldin, M.; Shats, JE.; Culbertson, BM.; Pittman, CU., editors. Plenum; New York: 1996. p. 481-489.

[27]. White, PD.; Chan, WC. Fmoc Solid Phase Peptide Synthesis: a Practical Approach. Oxford University Press; New York: 2000.

[28]. Edelhoch H. Spectroscopic determination of tryptophan and tyrosine in proteins. Biochemistry. 1967; 6:1948–1954. [PubMed: 6049437]

[29]. Liang Q, Ananias DC, Long EC. Ni(II)•Xaa-Xaa-His induced DNA cleavage: Deoxyribose modification by a common "activated" intermediate derived from $KHSO_5$, MMPP, and H_2O_2. J. Am. Chem. Soc. 1998; 120:248–257.

[30]. Kanemasa, S.; Oderaotashi, Y.; Yamamoto, H.; Tanaka, J.; Wada, E. Spartan '02. Wavefunction, Inc., 18401 Von Karman, Suite 370; Irvine, CA:

[31]. Sybyl 7.2. Tripos, Inc; St. Louis, MO:

[32]. Mohamadi F, Richards NGJ, Guida WC, Liskamp R, Lipton M, Caufield C, Chang G, Hendrickson T, Still WC. MacroModel - an integrated software system for modeling organic and bioorganic molecules using molecular mechanics. J. Comput. Chem. 1990; 11:440–467.

[33]. Case, DA.; Pearlman, DA.; Caldwell, JW.; Cheatham, TE., III; Wang, J.; Ross, WS.; Simmerling, CL.; Darden, TA.; Merz, KM.; Stanton, RV.; Cheng, AL.; Vincent, JJ.; Crowley, M.; Tsui, V.; Gohlke, H.; Radmer, RJ.; Duan, Y.; Pitera, J.; Massova, I.; Seibel, GL.; Singh, UC.; Weiner, PK.; Kollman, PA. AMBER 7. University of California; San Francisco: 2002.

[34]. Fang Y-Y, Ray BD, Claussen CA, Lipkowitz KB, Long EC. Ni(II)•Arg-Gly-His-DNA interactions: Investigation into the basis for minor-groove binding and recognition. J. Am. Chem. Soc. 2004; 126:5403–5412. [PubMed: 15113212]

[35]. Ananias DC, Long EC. DNA strand scission by dioxygen + light-activated cobalt metallopeptides. Inorg. Chem. 1997; 36:2469–2471. [PubMed: 11669890]

[36]. Ananias DC, Long EC. Highly selective DNA modification by ambient O_2-activated Co(II)•Lys-Gly-His metallopeptides. J. Am. Chem. Soc. 2000; 122:10460–10461.

[37]. Hawkins CJ, Martin J. Cobalt(III) complex of glycylglycyl-histidine: Preparation, characterization, and conformation. Inorg. Chem. 1983; 22:3879–3883.

[38]. Bal W, Djuran MI, Margerum DW, Gray ET, Mazid MA, Tom RT, Nieboer E, Sadler PJ. Dioxygen-induced decarboxylation and hydroxylation of [Ni^{II}(glycyl-glycyl-L-histidine)] occurs via Ni^{III}: X-ray crystal structure of [Ni^{II}(glycyl-glycyl-hydroxy-D,L-histamine)]•$3H_2O$. J. Chem. Soc., Chem. Commun. 1994:1889–1890.

[39]. Long EC. Ni(II)•Xaa-Xaa-His metallopeptide-DNA/RNA interactions. Acc. Chem. Res. 1999; 99:827–836.

[40]. Long, EC.; Fang, Y-Y.; Lewis, MA. Bioinorganic Chemistry: Cellular Systems and Synthetic Models. Long, EC.; Baldwin, MJ., editors. Vol. Volume 1012. American Chemical Society; Washington, D. C.: 2009. p. 219-241.ACS Symposium Series
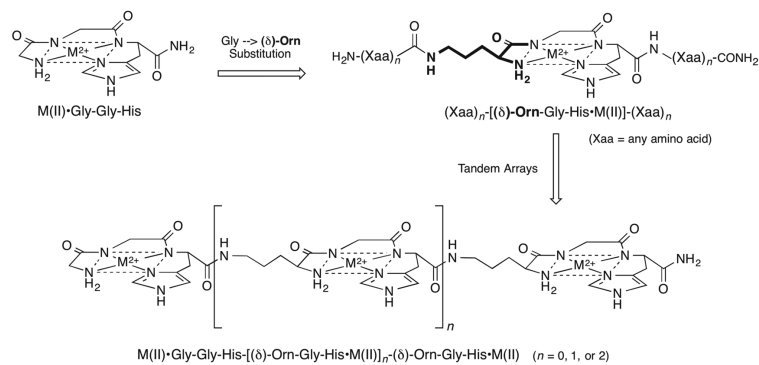
Fig. (1).
Structure of M(II)•Gly-Gly-His and illustration of the (δ)-Orn strategy to permit the transformation of amino-terminal Gly-Gly-His metal binding motifs into a metal binding system that can be placed at any location in a peptide or in tandem arrays; Orn substitution for Gly_1 (top) shown in bold.
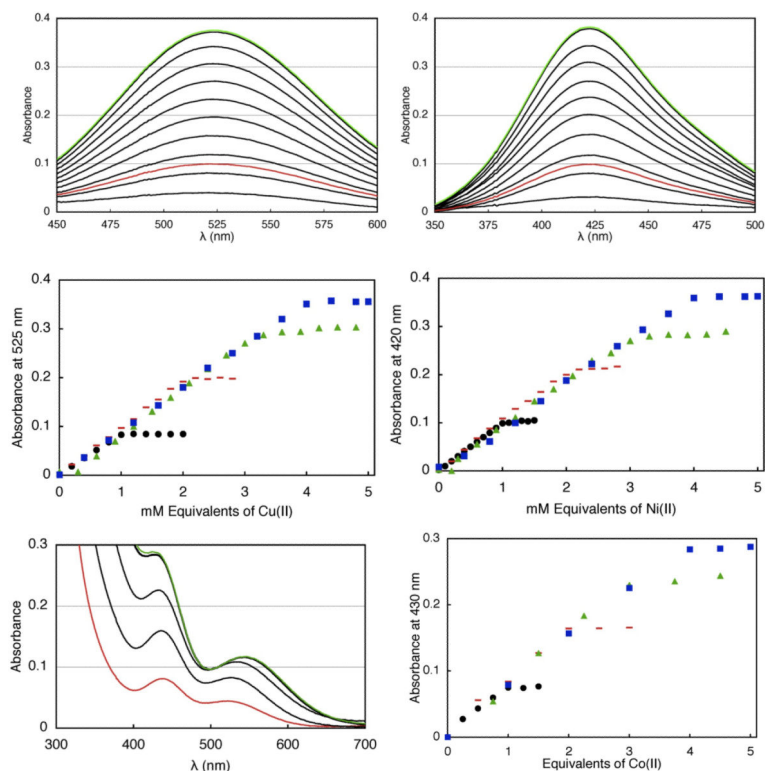
Fig. (2).

Top panels: Titrations of 1 mM solutions of peptide **4** (containing 4 metal binding sites) with Cu^{2+} (left) and Ni^{2+} (right) monitored by UV-vis spectroscopy. Titrations in these top panels illustrate the increasing absorbance observed upon the addition of 0.4 equivalents of metal ion (per increment of addition) up to four total equivalents (relative to peptide **4**). Each black spectrum in the left and right top panels illustrates the absorbance increase observed upon a 0.4 equivalent addition of metal ion (Cu or Ni). The lowest black absorbance spectrum represents the absorbance observed upon the addition of 0.4 equivalents of added metal, the next highest black spectrum represents the addition of 0.8 equivalents of added metal, the next black spectrum represents the addition of 1.2 equivalents, etc. In total, there are 10 stacked black spectra (10×0.4 equivalents = 4 total equivalents of added metal). Given that each peptide **4** contains 4 metal binding sites, a 1 mM solution of **4** contains 4 mM metal binding sites, thus requiring 4 full equivalents of added metal ion (relative to peptide) to achieve binding saturation, as observed. The green absorbance spectrum in each top panel (overlapping with the black spectrum of highest absorbance) illustrates the absorbance observed upon addition of one further full equivalent of metal ion (**4**:M^{2+} = 1:5); no further increase in absorbance was observed, metal binding saturation was achieved upon 4 added equivalents. For comparison, the red absorbance superimposed on each plot illustrates the absorbance observed from a 1:1 mixture of Cu(II)•**1** or Ni(II)•**1** (1 mM). *Middle panels:* UV-Vis titrations of peptides **1**–**4** with Cu^{2+} (left) and Ni^{2+} (right). Titrations illustrate the increasing absorbance observed at 525 nm (Cu) or 420 nm (Ni) upon the addition of 0.4 equivalents of metal ion per increment of addition (black: **1**; red: **2**; green: **3**; blue: **4**); breakpoints in each titration occur upon saturation of each metal binding site. *Bottom panels:* UV-visible absorbance analysis of

peptide **4** (left) in the presence of one (red), two, three, four, or five (green) equivalents of Co and titrations of peptides **1**–**4** with Co (right): black, **1**; red, **2**; green, **3**; and blue, **4**). In each case, Co^{2+} binding was followed by *in situ* generation of Co(III)-metallated peptides prior to spectroscopic analysis.
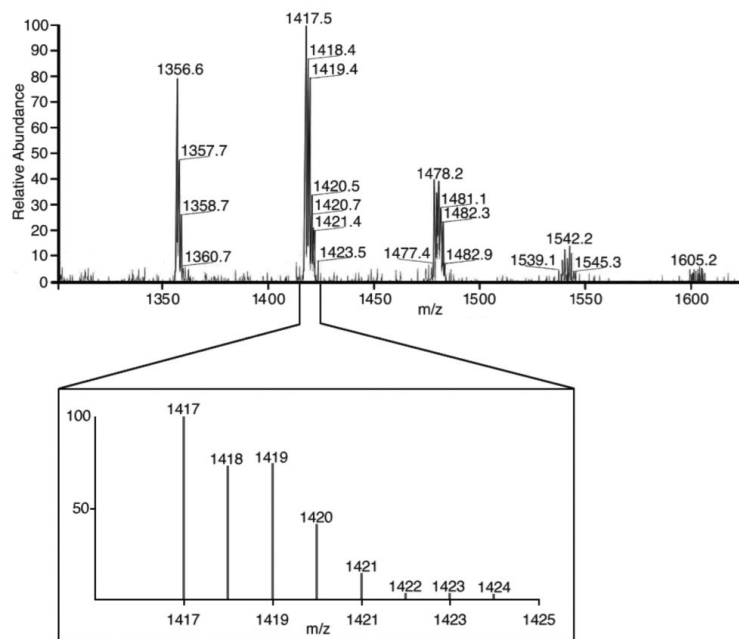
Fig. (3).
ESI-MS analysis of Cu(II)-bound peptide **4** at a ratio of Cu^{2+} to metal binding site of 3:4. The expansion shown illustrates the predicted isotopic distribution for one bound equivalent of Cu to **4**.
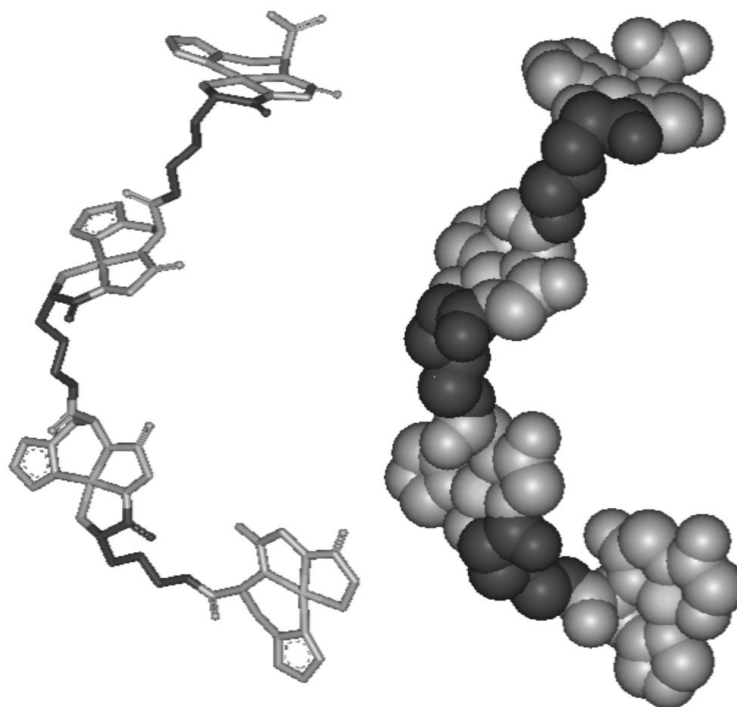
Fig. (4).
Molecular models representing the average structure of Ni(II)$_4$•Gly-Gly-His-(δ)-Orn-Gly-His-(δ)-Orn-Gly-His-(δ)-Orn-Gly-His determined by MD simulations.
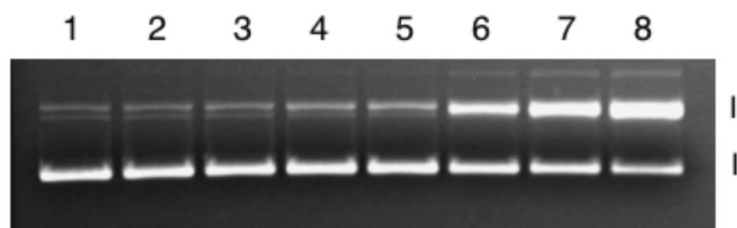
Fig. (5).

Analysis of the DNA cleavage activity of Ni(II)•Gly-Gly-His, Ni(II)$_2$•Gly-Gly-His-(δ)-Orn-Gly-His and Ni(II)$_3$•Gly-Gly-His-(δ)-Orn-Gly-His-(δ)-Orn-Gly-His. All reactions contained 30 μM ΦX174 RF DNA (base pair concentration) in 10 mM Na-cacodylate buffer, pH 7.5. Lane 1: reaction control, DNA alone; Lane 2: reaction control, DNA, 30 μM Ni^{2+}, 30 μM KHSO$_5$; Lane 3: reaction control, DNA, 30 μM KHSO$_5$, 30 μM Gly-Gly-His; Lane 4: reaction control, DNA, 30 μM KHSO$_5$, 15 μM Gly-Gly-His-(δ)-Orn-Gly-His; Lane 5: reaction control, DNA, 30 μM KHSO$_5$, 10 μM Gly-Gly-His-(δ)-Orn-Gly-His-(δ)-Orn-Gly-His; Lane 6: 30 μM Ni^{2+}, 30 μM KHSO$_5$, 30 μM Gly-Gly-His; Lane 7: 30 μM Ni^{2+}, 30 μM KHSO$_5$, 15 μM Gly-Gly-His-(δ)-Orn-Gly-His; Lane 8: 30 μM Ni^{2+}, 30 μM KHSO$_5$, 10 μM Gly-Gly-His-(δ)-Orn-Gly-His-(δ)-Orn-Gly-His.